Mixed-spin Ising model and compensation temperature

Maurício Godoy, Vanessa Souza Leite, and Wagner Figueiredo*
Departamento de Física, Universidade Federal de Santa Catarina, 88040-900 Florianópolis, Santa Catarina, Brazil
(Received 12 September 2003; revised manuscript received 18 November 2003; published 27 February 2004)

We presented a study of the magnetic properties of a mixed-spin Ising ferrimagnetic model on a hexagonal lattice. The lattice is formed by alternate layers of spins $\sigma = 1/2$ and $S = 1$. For this spin arrangement, any spin at one lattice site has two nearest-neighbor spins on the same sublattice, and four on the other sublattice. The intersublattice interaction is antiferromagnetic. The compensation point is a special point that appears below the critical temperature, for which the sublattice magnetizations cancel each other. We employed mean-field calculations and Monte Carlo simulations to find the compensation point of the model. The role of the different interactions in the Hamiltonian is explored. When the intrasublattice interaction for the σ spins exceeds a minimum value, which depends on the other parameters of the Hamiltonian, a compensation point is possible. We have also shown that the phase diagram in the plane magnitude of S-S exchange interactions versus crystal-field intensity exhibits a very narrow region of compensation points.

DOI: 10.1103/PhysRevB.69.054428 PACS number(s): 05.50.+q, 75.10.Hk, 75.40.Mg, 75.50.Gg

I. INTRODUCTION

Ferrimagnetic systems have been the object of a large number of experimental and theoretical studies, because of their great potential for technological applications, such as the high-density magneto-optical recording.[1,2] Mixed-spin Ising systems were introduced as the simplest models that can exhibit a ferrimagnetic order and compensation points. These systems have been studied by effective-field theories,[3,4] renormalization-group calculations,[5–7] and Monte Carlo simulations.[8,9]

In a ferrimagnetic material the different temperature dependences of the sublattice magnetizations cause the appearance of compensation points. The compensation temperature is a temperature below the critical one, for which the total magnetization is zero.[10] It has been found that at this point some physical properties present a peculiar behavior. For instance, a divergence in the coercivity is observed:[2,11,12] at the compensation point only a small driving field is required to reverse the sign of the magnetization of the system. Because some ferrimagnetic materials have a compensation temperature (T_{comp}) near room temperature, they are of fundamental importance in the area of the thermomagnetic recording devices.[2,13]

The presence of a compensation point in the mixed-spin models was already investigated on the square and honeycomb lattices.[3,8,9] In these lattice models only the σ-S interactions were considered between nearest-neighbor spins. Then, a mean-field calculation predicts a compensation point only for a very narrow region of negative values of the crystal-field parameter. On the other hand, by Monte Carlo simulations, it was demonstrated that it is necessary to include a ferromagnetic interaction between σ spins, which are next-nearest neighbors in a bipartite lattice, in order to have a compensation point.

In the layered mixed-spin Ising model on the hexagonal lattice, investigated in this work, only nearest-neighbor interactions between spins are sufficient to predict a compensation point. If this model would be extended to three dimensions it could describe some properties of real ferrimagnetic materials. For instance, the work of Chern *et al.*[14] reports some measurements of the compensation point and phase diagram of Fe_3O_4/Mn_3O_4 superlattices, which is a system grown by a deposition of alternate layers of Fe_3O_4 and Mn_3O_4 coupled antiferromagnetically. In the remainder of this work, we present in Sec. II the model and the dynamic equations for the sublattice magnetizations in the mean-field approximation. We next, in Sec. III, describe the Monte Carlo simulations. In Sec. IV we show our results, and finally, we present our conclusions in Sec. V.

II. THE MODEL

We consider a mixed-spin ferrimagnetic Ising model on a hexagonal lattice. The two different types of spins are described by Ising variables, which can take the values $\sigma = \pm 1/2$ and $S = \pm 1, 0$. The two different spins are distributed in alternate layers of a hexagonal lattice, as we can see in Fig. 1.

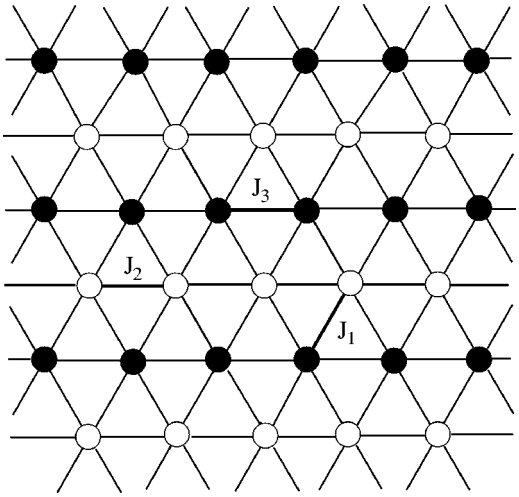

FIG. 1. Schematic representation of the hexagonal lattice. The lattice is formed by alternate layers of σ (open circles) and S (solid circles) spins.

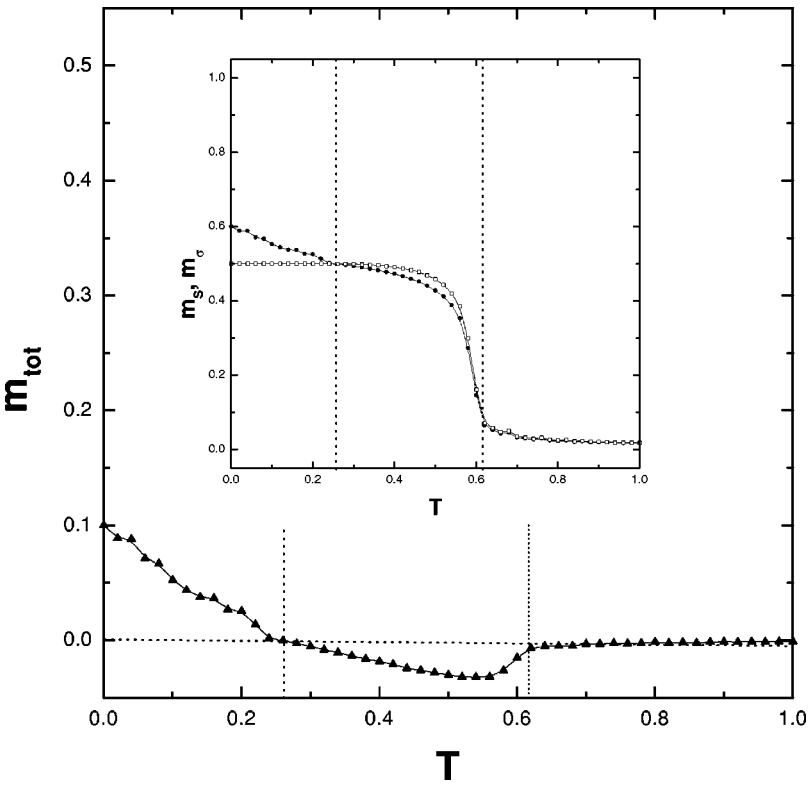

FIG. 2. Sublattice and total magnetizations as a function of temperature obtained by Monte Carlo simulations for $J_2=-J_1$, $J_3=1.05J_1$, and $D=-0.75|J_1|$. The inset shows the sublattice magnetizations. T_{comp} and T_c are shown in the figure.

The Hamiltonian model for the system is

$$\mathcal{H}=-J_1\sum_{\langle ij\rangle} S_i\sigma_j-J_2\sum_{\langle ij\rangle}\sigma_i\sigma_j-J_3\sum_{\langle ij\rangle} S_iS_j-D\sum_i S_i^2, \tag{1}$$

where J_1, J_2, and J_3 are the exchange couplings between nearest-neighbor pairs of spins σ-S, σ-σ, and S-S, respectively. The parameter J_1 will be taken negative in all the subsequent analyses, that is, the intersublattice coupling is antiferromagnetic. D is the crystal field that acts only at the S spin sites. In order to study this model in the mean-field approximation, we consider the dynamic equations for the average sublattice magnetizations,

$$m_\sigma(t)=\sum_{\langle\sigma,S\rangle}\sigma P(\sigma,S;t) \tag{2}$$

and

$$m_S(t)=\sum_{\langle\sigma,S\rangle} SP(\sigma,S;t), \tag{3}$$

where the sums are over all the possible spin configurations, and $P(\sigma,S;t)$ is the probability to find the system in a give state (σ,S) at time t.

The time evolution for the state probability is obtained from the master equation,[15]

$$\frac{d}{dt}P(\sigma,S;t)=\sum_{\sigma',S'}[W(\sigma',S'\to\sigma,S)P(\sigma',S';t) - W(\sigma,S\to\sigma',S')P(\sigma,S;t)], \tag{4}$$

where $W(\sigma,S\to\sigma',S')$ is the transition rate from the state (σ,S) to the state (σ',S'). In this work, we assume that

$$W(\sigma,S\to\sigma',S')=W(\sigma,S\to\sigma',S)+W(\sigma,S\to\sigma,S'). \tag{5}$$

For this transition rate we also assume the one-spin-flip Glauber dynamics,[16] that is,

$$\begin{aligned}W(\sigma,S\to\sigma',S') &=\sum_{j=1}^{N}\delta_{\sigma_1,\sigma_1'}\cdots\delta_{\sigma_j,-\sigma_j'}\cdots\delta_{\sigma_N,\sigma_N'} \\ &\times\delta_{S_1,S_1'}\cdots\delta_{S_k,S_k'}\cdots\delta_{S_N,S_N'}w_j(\sigma') \\ &+\sum_{k=1}^{N}\delta_{\sigma_1,\sigma_1'}\cdots\delta_{\sigma_j,\sigma_j'}\cdots\delta_{\sigma_N,\sigma_N'} \\ &\times\delta_{S_1,S_1'}\cdots\delta_{S_k,\tilde{S}_k'}\cdots\delta_{S_N,S_N'}w_k(\tilde{S}'),\end{aligned} \tag{6}$$

where $w_j(\sigma')$ and $w_k(\tilde{S}')$ are the flipping probabilities for the spins on the σ and S sublattices, per unit time, respectively.

Using Eqs. (4) and (6) we find

$$\frac{d}{dt}\langle\sigma_j\rangle=-2\langle\sigma_j w_j(\sigma)\rangle \tag{7}$$

and

$$\frac{d}{dt}\langle S_k\rangle=\langle(S_k'-S_k)w_k(S)\rangle. \tag{8}$$

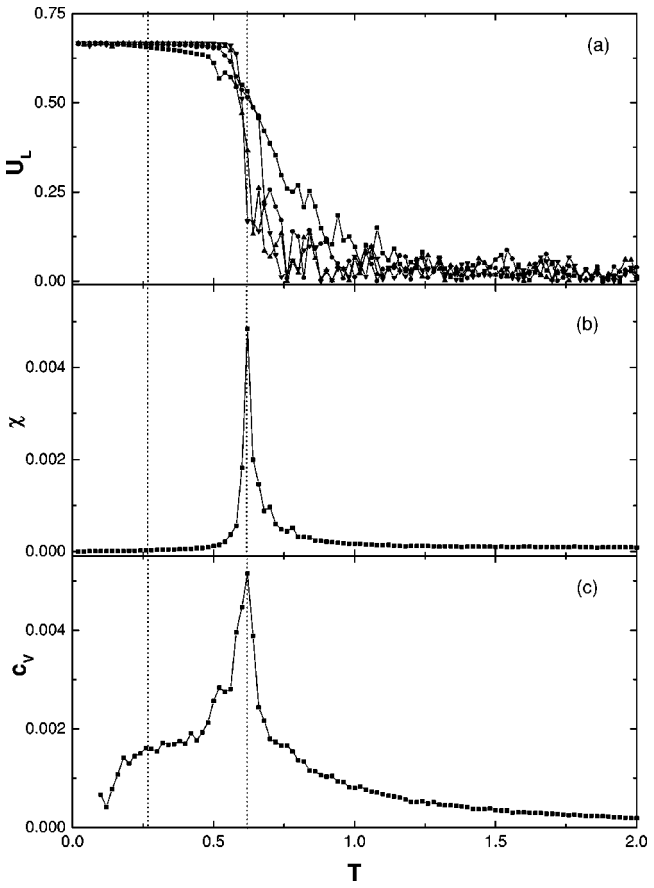

FIG. 3. (a) Fourth-order cumulants for the hexagonal lattices with $L=8$ (squares), $L=16$ (circles), $L=32$ (up triangles), and $L=64$ (down triangles). (b) Susceptibility, and (c) specific heat as a function of temperature for the same parameters of Fig. 2 and for $L=64$. T_{comp} and T_c are shown in the figure.

The spins of the σ sublattice flip with a probability per unit time given by the normalized Boltzmann factor,[17]

$$w_j(\sigma)=\frac{\exp(-\beta\Delta\mathcal{H})}{\sum_{\sigma'}\exp(-\beta\Delta\mathcal{H})}, \tag{9}$$

where $\beta=1/k_BT$, k_B is the Boltzmann constant and T is the absolute temperature. $\Delta\mathcal{H}$ is the energy change of the system when one spin of the σ sublattice flips. If the spin σ_j flips,

$$\Delta\mathcal{H}(\sigma_j)=-2\sigma_j\left(J_1\sum_k S_k+J_2\sum_k \sigma_k\right), \tag{10}$$

and

$$w_j(\sigma)=\frac{\exp[-\beta\Delta\mathcal{H}(\sigma_j)]}{1+\exp[-\beta\Delta\mathcal{H}(\sigma_j)]}. \tag{11}$$

In a similar way, we define the transition rates for the spins on the S sublattice. We have

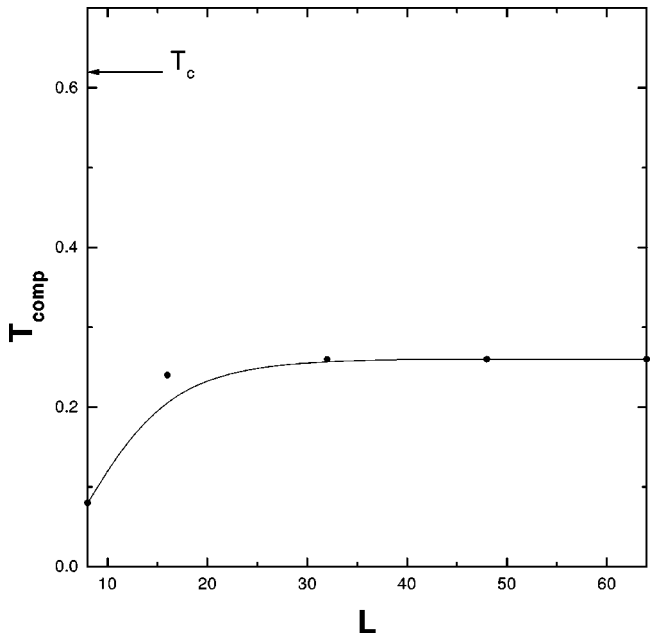

FIG. 4. Compensation temperatures determined for different lattice sizes and for the same parameters of Fig. 2. T_c is also shown in the figure.

$$w_k(1\to 0)=w_k(-1\to 0)=\frac{\exp(-\beta D)}{2\cosh(\beta\alpha)+\exp(-\beta D)}, \tag{12}$$

$$w_k(1\to -1)=w_k(0\to -1)=\frac{\exp(-\beta\alpha)}{2\cosh(\beta\alpha)+\exp(-\beta D)}, \tag{13}$$

$$w_k(-1\to 1)=w_k(0\to 1)=\frac{\exp(\beta\alpha)}{2\cosh(\beta\alpha)+\exp(-\beta D)}, \tag{14}$$

where $\alpha=J_1\Sigma_j\sigma_j+J_3\Sigma_jS_j$.

In the mean-field approximation, the probability of finding the system in the state (σ,S) at time t is equal to the product of the probabilities of the independent spin states:

$$P(\sigma,S;t)=\prod_{j,k}P(\sigma_j,S_k;t)=\prod_{j,k}P(\sigma_j;t)P(S_k;t), \tag{15}$$

where for the probabilities of the individual spin states we write,[18]

$$P(\sigma_j;t)=\tfrac{1}{2}(1+4\sigma_j m_\sigma), \tag{16}$$

$$P(S_k;t)=1-S_k^2+\tfrac{1}{2}S_k m_S-(1-\tfrac{3}{2}S_k^2)q_k, \tag{17}$$

where $q_k=\Sigma_{\langle\sigma,S\rangle}S_k^2P(\sigma,S;t)$. Introducing these probabilities in the expressions for the transition rates, we finally arrive at the equations of motion for the sublattice magnetizations in the mean-field approximation:

$$\frac{d}{dt}m_\sigma=-m_\sigma+\frac{1}{2}\tanh[\beta(2J_1m_S+J_2m_\sigma)] \tag{18}$$

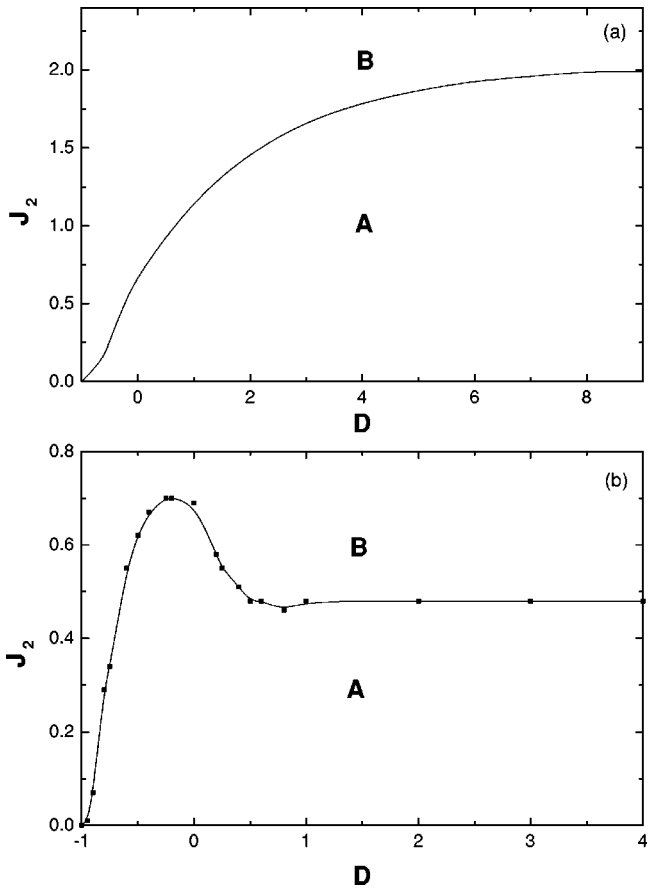

FIG. 5. Minimum value of J_2 for the appearance of a compensation point as a function of the crystal field, D. (a) Mean-field calculations for $J_3=J_1$, and (b) Monte Carlo simulations for $J_3=0.98J_1$. Region A, $m_S>m_\sigma$ for $T<T_c$, and B is the region where a compensation point appears.

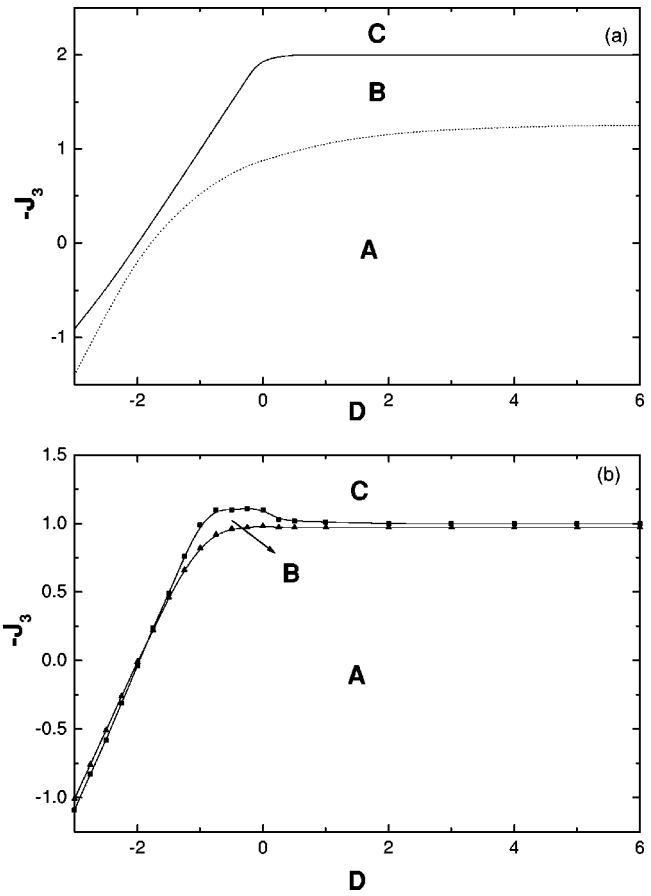

FIG. 6. Range of values of J_3 giving rise to the compensation points, as a function of the crystal field D for $J_2=-J_1$. (a) Mean-field calculations, and (b) Monte Carlo simulations. B is the only region where we can have compensation points. For the regions A and C, we always have $m_S>m_\sigma$ and $m_\sigma>m_s$, respectively.

and

$$\frac{d}{dt}m_S=-m_S+\frac{2\sinh[2\beta(2J_1m_\sigma+J_3m_S)]}{2\cosh[2\beta(2J_1m_\sigma+J_3m_S)]+\exp(-\beta D)}. \tag{19}$$

We solved this system of equations for the equilibrium states as a function of the temperature, for different values of the Hamiltonian parameters.

III. MONTE CARLO SIMULATIONS

The model described in the preceding section was simulated by using standard importance sampling techniques. The initial configurations were taken randomly. We try to flip the spins according to the heat-bath algorithm,[19] and in each Monte Carlo step (MCS), we performed L^2 trials to flip the spins. We considered hexagonal lattices (as seen in Fig. 1) with L^2 sites, and applied periodic boundary conditions. Most of the data were obtained for $L=64$, but we also considered lattices of linear sizes $L=8$, 16, 32, 48, and 128. For $L=64$, we performed around 4000 MCS, where the first 1000 were discarded for the thermalization process. In order to get reliable results, we also considered averages over 100 different samples in our calculations. Although not shown in the figures, the error bars are smaller than the symbol sizes.

Our algorithm calculates the σ and S sublattice magnetizations, defined as

$$m_\sigma=\frac{2}{L^2}\left\langle\sum_j \sigma_j\right\rangle, \tag{20}$$

$$m_S=\frac{2}{L^2}\left\langle\sum_k S_k\right\rangle, \tag{21}$$

and the total magnetization

$$m_{tot}=\tfrac{1}{2}(m_\sigma+m_S). \tag{22}$$

The sums in j and k are over all the spins in the σ and S sublattices, respectively.

The total magnetization m_{tot} vanishes at the compensation temperature T_{comp}. Then, the compensation point can be determined by looking for the crossing point between the absolute values of the sublattice magnetizations. Therefore, at the compensation point, we must have

$$|m_\sigma(T_{comp})|=|m_S(T_{comp})| \tag{23}$$

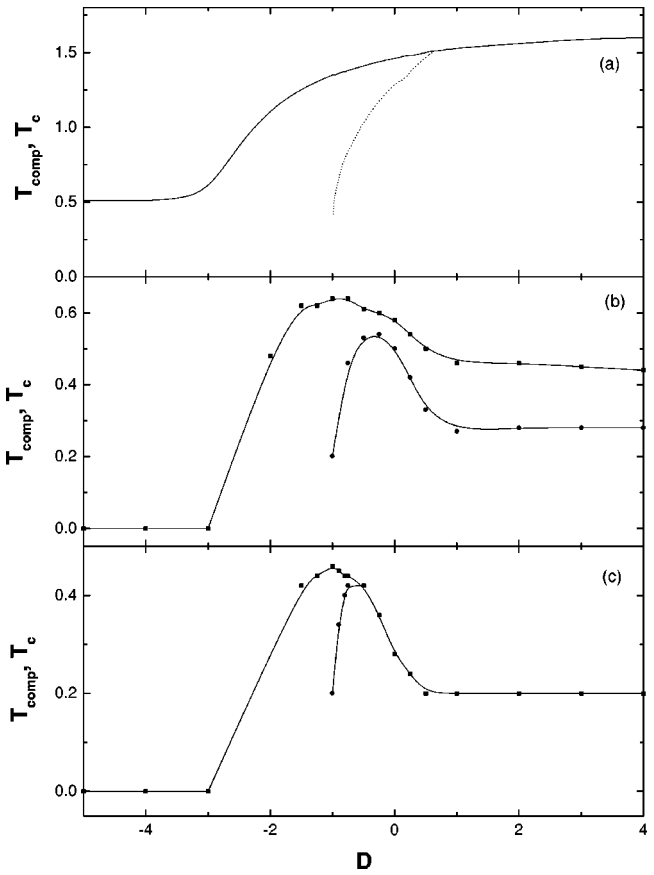

FIG. 7. Behavior of T_{comp} and T_c as a function of D. (a) Mean-field calculations for $J_2=-J_1$ and $J_3=J_1$, (b) Monte Carlo simulations for $J_2=-J_1$ and $J_3=0.98J_1$, and (c) Monte Carlo simulations for $J_2=-J_1$ and $J_3=0.40J_1$.

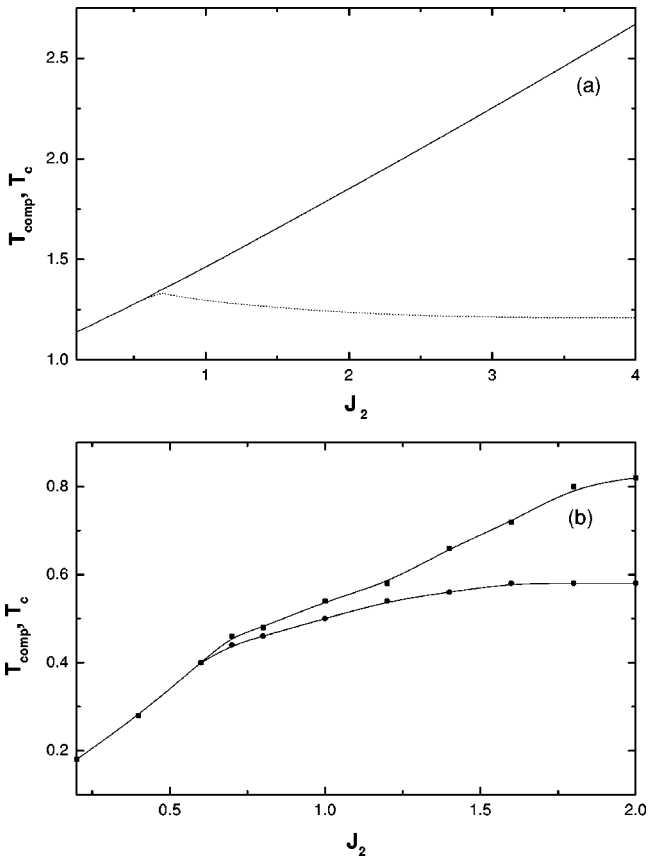

FIG. 8. Plots of T_{comp} and T_c as a function of J_2. (a) Mean-field calculations for $D=0$ and $J_3=J_1$, and (b) Monte Carlo simulations for $D=0$ and $J_3=0.98J_1$.

and

$$\mathrm{sgn}[m_\sigma(T_{comp})]=-\mathrm{sgn}[m_S(T_{comp})]. \tag{24}$$

We also require that $T_{comp}<T_c$, where T_c is the critical-point temperature.

These conditions show that at T_{comp}, the σ and S sublattice magnetizations cancel each other, whereas at T_c both are zero. To illustrate this property, we show in Fig. 2 the sublattice and total magnetizations as a function of the temperature for selected values of the Hamiltonian parameters, which lead to a compensation point. In this case, we have $J_2=-J_1$, $J_3=1.05J_1$, and $D=-0.75|J_1|$. We call attention that for this value of D, the S sublattice magnetization is not saturated at $T=0$. The simulation points can be obtained down to $T=0.02|J_1|/k_B$ using safely 4000 Monte Carlo steps as explained before. For temperatures below this, the time for thermalization is too long and the simulation points are extrapolated to $T=0$ to coincide with the mean-field values. Then, from the Monte Carlo simulations of Fig. 2, we have $T_{comp}=(0.26\pm0.02)|J_1|/k_B$ for the compensation point, and $T_c=(0.62\pm0.02)|J_1|/k_B$, for the transition temperature.

In Fig. 3(a) we show the fourth-order cumulants for the same parameters of the Fig. 2, for lattices with L equal to 8, 16, 32 and 64. As can be seen in this figure, at the compensation point the model does not present any critical phenomenon; only at T_c the critical behavior is observed through the crossing of the cumulants. We see in Figs. 3(b) and 3(c) the plots of the susceptibility and specific heat as a function of temperature, for $L=64$, respectively. Once again, it is clear that these properties are regular functions at T_{comp}; only at T_c they display a singular behavior. The compensation point appears only due to the different dependences on temperature of the sublattice magnetizations and does not exhibit any special singularity. Figure 4 shows the different compensation temperatures as a function of the lattice size. We note that T_{comp} is not sensitive to the lattice size. This is the reason we performed the calculations for the lattice size $L=64$, when we are looking at the compensation point.

IV. RESULTS

We start our analysis by looking for the Hamiltonian parameters of the model for which a compensation point appears. As we will see below, the compensation point is present only for a ferromagnetic intrasublattice coupling between σ spins. Besides, we also require an antiferromagnetic coupling between spins on the S sublattice or a negative value for the crystal-field parameter. All these features are necessary in order for m_S to decrease faster than m_σ when the temperature increases.

Figure 5(a) shows the minimum value of the ferromag-

netic intrasublattice interaction between σ spins, J_2, as a function of D, in the mean-field approximation for $J_3=J_1$. For values of J_2 below the minimum, m_S is always larger than m_σ for any value of $T<T_c$. The minimum value depends on the intensity of the crystal-field parameter D. The minimum value of J_2, for which a compensation point appears, is an increasing function of D. As D decreases, the sublattice magnetization m_S decays faster, and the crossing point of the two sublattice magnetizations moves to lower temperatures. For the exchange parameters, J_1 and J_3 considered in this plot, the model does not exhibit any compensation point for $D<-1.0|J_1|$. In this region, the sublattice magnetization m_S is lower than m_σ for any value of the intrasublattice interaction in the σ sublattice.

In Fig. 5(b) we present the minimum value of J_2 obtained through Monte Carlo simulations for $J_3=0.98J_1$. Comparing this plot with the one found in the mean-field calculation, we observe a different behavior in the range of values $0<D<0.50|J_1|$, where the minimum value of J_2 decreases with D. We believe that this behavior must be attributed to a dimensional crossover of the model, once we observed that for $D<-3.0|J_1|$ the system is represented by a set of uncoupled chains of σ spins. Then, this behavior is not seen in the mean-field calculations because dimensional details are not captured at this level of approximation.

On the other hand, the antiferromagnetic intrasublattice interaction between spins at the S sublattice establishes two limits for the existence of a compensation point. Below the minimum value, the m_S does not decrease enough, and for any temperature below the critical, $m_S>m_\sigma$. Above the maximum value, the antiferromagnetic interaction between the S spins is too large that m_S is always lower than m_σ for any temperature below the critical one. Only in the region between these extreme values of J_3, a compensation point can appear. These limits depend on the value of D, as we can see in Fig. 6, for $J_2=-J_1$. Figures 6(a) and 6(b) give the mean field and simulation results, respectively. Monte Carlo simulations give a much more narrow range of J_3 values, for which the compensation point exists. For the upperbond curve of J_3, the simulations also predict a different behavior as a function of D in the range $-0.50|J_1|<D<0$, compared with the mean-field one.

The dependence of T_{comp} and T_c on the crystal-field parameter D is seen in Fig. 7. Figure 7(a) displays the mean-field results for the parameters $J_2=-J_1$ and $J_3=J_1$. As we can see, for $D<-1.0|J_1|$ the system does not exhibit any compensation point. However, when D increases, T_{comp} and T_c both increase, and T_{comp} approaches to T_c. For $D=0.6|J_1|$, we have $T_{comp}=T_c$. This picture is also observed in Fig. 6(a) for $J_3=J_1$. Therefore, only in the range $-1.0|J_1|<D<0.6|J_1|$ there is a compensation point. Figure 7(b) shows the simulation results for $J_2=-J_1$ and $J_3=0.98J_1$. In this figure only for $D<-1.0|J_1|$ there is not a compensation point. The value $J_3=0.98J_1$ belongs to the narrow region of Fig. 6(b) where, for $D>-1.0|J_1|$, a compensation point is possible to be realized. Simulations for $J_3=0.4J_1$ give the curves shown in Fig. 7(c). In this case, there is a compensation point only in a very narrow range of values of D, which can also be appreciated in Fig. 6(b). As observed in Figs. 5 and 6, the simulation results shown in Figs. 7(b) and 7(c), are qualitatively different for all $D>-1$ and quantitatively different for other D, from those seen in the mean-field calculations.

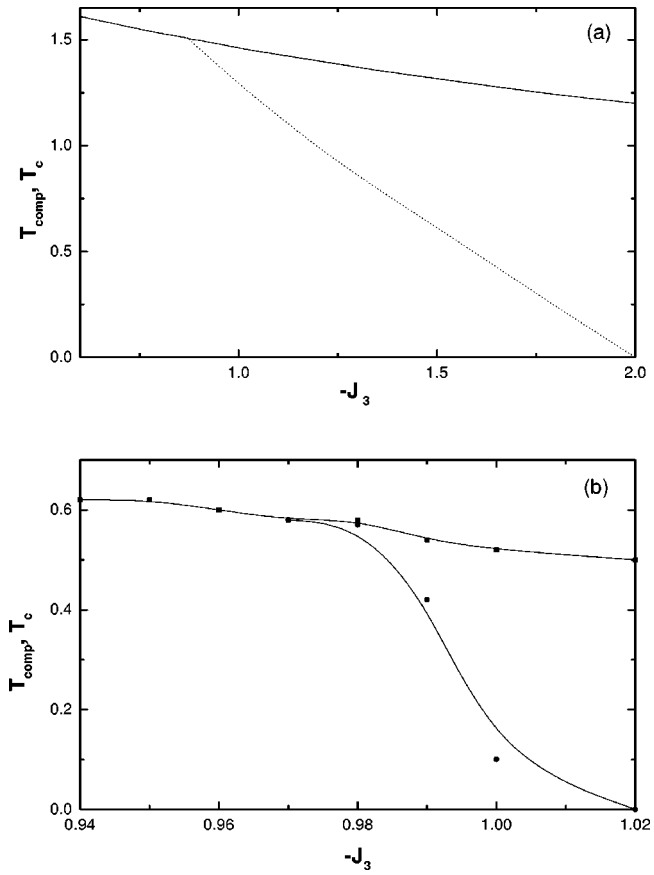

FIG. 9. Plots of T_{comp} and T_c as a function of J_3, for $D=0$ and $J_2=-J_1$. (a) Mean-field calculations, and (b) Monte Carlo simulations.

Figure 8 exhibits the compensation and critical temperatures as a function of J_2 for $D=0$. Figure 8(a) gives the mean-field results for $J_3=J_1$ and Fig. 8(b) the simulation results for $J_3=0.98J_1$. As we can see, a compensation point appears only when a minimum value of J_2 is reached. The critical temperature always increases with J_2. As to be expected, increasing J_2 above its minimum value, the σ sublattice keeps ordered up to high temperatures. However, as m_S is almost constant, the crossing point between m_σ and m_S changes a little, and T_{comp} is nearly constant.

Finally, we plotted in Fig. 9, T_{comp} and T_c as a function of the antiferromagnetic intrasublattice interaction J_3. In these plots we used $J_2=-J_1$ and $D=0$. Figures 9(a) and 9(b) represent the mean-field and simulation results, respectively. As we can see, T_{comp} and T_c are both decreasing functions of J_3. These results were expected because increasing J_3, we disorder the S sublattice. That is, increasing J_3, m_S decreases and a lower temperature is needed for which $m_\sigma=m_S$. Finally, at a given value of J_3, the compensation temperature goes to zero.

V. CONCLUSIONS

In this work we have considered mean-field calculations and Monte Carlo simulations to study a mixed-spin Ising system, where the $\sigma = 1/2$ and $S = 1$ spins occupy alternate layers of a hexagonal lattice. The Hamiltonian model includes intersublattice, intrasublattice, and crystal-field interactions. The intersublattice interaction is considered antiferromagnetic in order to have a simple but an interesting model of a ferrimagnetic system. We have investigated the role of the different interactions in the Hamiltonian to predict a compensation point in the model. Our results show that, the compensation point appears only when the intrasublattice interaction between spins in the σ sublattice is ferromagnetic. There is a minimum value of this coupling, which depends on the other Hamiltonian parameters, for the appearance of a compensation point. The intrasublattice interaction between spins in the S sublattice and the crystal-field parameter must contribute to decrease the magnetization of the S sublattice for the appearance of a compensation point. We also have shown that there is a very narrow range of values of the coupling between S spins where it is possible to find a compensation point. We have seen that the mean-field calculations give results that disagree from those obtained by Monte Carlo simulations. They are quantitatively different for all the values of the Hamiltonian parameters we have considered, and are qualitatively different for a range of these parameters. Therefore, this layered spin model predicts a compensation point by taking into account only nearest-neighbor spin interactions. For the usual bipartite lattice, we also need to include next nearest-neighbor interactions to have a compensation point.

ACKNOWLEDGMENTS

The authors acknowledge financial support by the Brazilian agencies CNPq, CAPES, and FUNCITEC.

*Email address: wagner@fisica.ufsc.br

[1] *Magnetic Molecular Materials*, Vol. 198 of *NATO Science Series E: Applied Sciences*, edited by D. Gatteschi, O. Kahn, J.S. Miller, and F. Palacio (Kluwer Academic, Dordrecht, 1991).
[2] H.P.D. Shieh and M.H. Kryder, Appl. Phys. Lett. **49**, 473 (1986).
[3] T. Kaneyoshi, Solid State Commun. **70**, 975 (1989); Physica A **205**, 677 (1994).
[4] A.F. Siqueira and I.P. Fittipaldi, J. Magn. Magn. Mater. **54**, 678 (1986).
[5] S.G.A. Quadros and S.R. Salinas, Physica A **206**, 479 (1994).
[6] H.F. Verona de Resende, F.C. S Barreto, and J.A. Plascak, Physica A **149A**, 606 (1988).
[7] B. Boechat, R.A. Filgueiras, C. Cordeiro, and N.S. Branco, Physica A **304**, 429 (2002).
[8] G.M. Buendia and J.A. Liendo, J. Phys.: Condens. Matter **9**, 5439 (1997).
[9] G.M. Buendia, M.A. Novotny, and J. Zhang, in *Springer Proceedings in Physics on Computer Simulation Studies in Condensed-Matter Physics VII*, edited by D.P. Landau, K.K. Mon, and H.B. Schttler (Springer-Verlag, Berlin, 1994).
[10] L. Néel, Ann. Phys. **3**, 137 (1948).
[11] G.A.N. Connel, R. Allen, and M. Mansuripur, J. Appl. Phys. **53**, 7759 (1982).
[12] J. Ostoréro, M. Escorne, A.P. Guegan, F. Soulette, and H. Le Gall, J. Appl. Phys. **75**, 6103 (1994).
[13] M. Mansuripur, J. Appl. Phys. **61**, 1580 (1987).
[14] G. Chern, L. Horng, W.K. Shieh, and T.C. Wu, Phys. Rev. B **63**, 094421 (2001).
[15] T. Tomé and M.J. de Oliveira, Phys. Rev. A **40**, 6643 (1989).
[16] R.J. Glauber, J. Math. Phys. **4**, 294 (1963).
[17] K. Binder, *Monte Carlo Methods in Statistical Physics* (Springer, Berlin, 1979).
[18] M. Godoy and W. Figueiredo, Phys. Rev. E **61**, 218 (1999).
[19] D.P. Landau and K. Binder, *A Guide to Monte Carlo Simulations in Statistical Physics* (Cambridge University Press, United Kingdom, 2000).